Environ Earth Sci (2011) 63:311–320
DOI 10.1007/s12665-010-0714-0

ORIGINAL ARTICLE

Atmospheric pollution indicated by trace elements in snow from the northern slope of Cho Oyu range, Himalayas

Yaping Liu · Shugui Hou · Sungmin Hong · Soon-Do Hur · Khanghyun Lee · Yetang Wang

Received: 28 July 2009 / Accepted: 11 August 2010 / Published online: 3 September 2010

Abstract Samples collected from a 0.87 m snow pit at a high altitude site in the Cho Oyu range, Himalayas were measured for V, Cr, Mn, Co, Ni, Cu, Zn, As, Rb, Sr, Cd, Sn, Sb, Ba, Tl, Pb, Bi, Th, and U using inductively coupled plasma mass spectrometry. In addition, major ions, oxygen stable isotopes, and microparticles were also measured to assist the interpretation of seasonal variation of trace elements. The trace elements show a distinct seasonality, i.e., higher concentrations during the non-monsoon season than those during the monsoon season. Significant correlation is observed between Ba and the other trace elements. Crustal enrichment factor (EF_c) analysis indicates that V, Mn, Co, Ni, Rb, Sr, and Th originate mainly from crustal dust, while anthropogenic inputs make an important contribution to the other trace elements (i.e., Cu, Zn, As, Cd, Sn, Sb, Ti, Pb, Bi, and U). Evidence from air mass back trajectories suggests that atmospheric trace element pollution reaching the studied area is transported dominantly by Indian summer monsoon during the monsoon season, while it is transported mainly by the westerlies during the non-monsoon season.

Keywords Trace elements · Atmospheric pollution · Seasonal variation · Cho Oyu range · Air mass trajectory

Y. Liu · S. Hou (✉)
State Key Laboratory of Cryospheric Sciences, Cold and Arid Regions Environmental and Engineering Research Institute, Chinese Academy of Sciences, Lanzhou 730000, China
e-mail: shugui@lzb.ac.cn

S. Hong · S.-D. Hur · K. Lee
Korea Polar Research Institute,
Incheon 406-840, Republic of Korea

Y. Wang
Shandong Marine Fisheries Research Institute,
Yantai 264006, China

Present Address:
S. Hou
School of Geographic and Oceanographic Sciences,
Nanjing University, Nanjing 210093, China

Present Address:
S. Hong
Department of Oceanography, Inha University,
253 Yonghyun-dong, Nam-gu,
Incheon 402-751, Republic of Korea

Introduction

During the recent decades, data have shown that Greenland and Antarctic snow and ice preserve detailed records of ancient and modern atmospheric trace elements pollution related to anthropogenic emissions (Hong et al. 1996; Vallelonga et al. 2002). Greenland and Antarctic snow and ice records have provided distinct evidences that atmospheric pollution for various trace elements is at a regional to hemispherical or even global scale through long-range transport and dispersion (Murozumi et al. 1969; Boutron et al. 1991; Hong et al. 1994, 1996; Candelone et al. 1995; Wolff et al. 1999; Planchon et al. 2002). The time scale of the atmospheric pollution for trace elements has been dated back from the Greek, Roman, and Medieval times (Hong et al. 1994, 1996) to the post-Industrial Revolution period (Murozumi et al. 1969; Candelone et al. 1995). During the recent years, data on the occurrence of trace elements in snow and ice from high altitude alpine glaciers such as Alps, Bolivian ice cap, eastern Tienshan and Mt. Muztagh Ata in eastern Pamirs have also documented the atmospheric pollution for various trace elements (Van de Velde et al. 1998; Rosman et al. 2000; Barbante et al. 2004; Hong et al. 2004; Li et al. 2006a, b, 2007). These data play an important

role to assess with great clarity the ancient and modern atmospheric pollution for trace elements at a regional scale.

The Himalayas play an important role in shaping the regional scale atmospheric circulation patterns over Asia (Shrestha et al. 2000). In the Himalayan region, precipitation is caused mainly by moisture transported by Indian monsoon and/or local moisture from short travelled convective air mass during summer (June–September) (Stravisi et al. 1998), while moisture is transported by the westerlies during winter and spring (October–May), thus the Himalayan region represents an ideal site for studying the chemistry of long-range transported species. The emissions of air pollution species in Asia are increasing rapidly during the past decades, resulting in local air pollution (Foell et al. 1995). Indeed, Asia has been the largest source region of anthropogenic trace element emissions to the atmosphere in the world (Pacyna and Pacyna 2001). Very recently, the trace elements concentrations were measured in Himalayan snow/firn samples (Duan et al. 2007; Kang et al. 2007; Lee et al. 2008). Such data have provided important insights into seasonal variation and anthropogenic inputs of trace elements in the remote high-altitude atmosphere in the central Himalayas. However, available data focus on the Mt. Qomolangma (Everest) area and thus the spatial coverage is not sufficient to confirm that the observations are representative of the vast Himalayan region. Further studies on changes in the occurrence of trace elements in snow and ice at different sites in Himalayas are necessary to characterize their seasonal variations, and to better understand the anthropogenic perturbation of atmospheric trace elements in this region.

First, the data of trace elements in successive snow pit samples on the northern slope of Cho Oyu in central Himalayas are presented. The main purpose of the present work is to expand the knowledge of the temporal and spatial characterizations of trace elements in high Himalayan regions to evaluate trace element pollution related to anthropogenic sources in atmospheric environment of Cho Oyu and to give a source consideration through applying the HYSPLIT 4.8 model to identify possible source regions of trace elements.

Methodology

Sampling site

Cho Oyu is the sixth highest peak on earth (8,201 m a.s.l.). On 7 October 2005, snow pit samples were collected at the Gyabrag (Jiabula) Glacier (28°10′41″N, 86°38′19″E, 6,303 m a.s.l.) on the northern slope of Cho Oyu (Fig. 1a). The sampling was performed before any other scientific operation (e.g., ice core drilling) prevented potential pollution, e.g., from gasoline electrical generator. A shallow

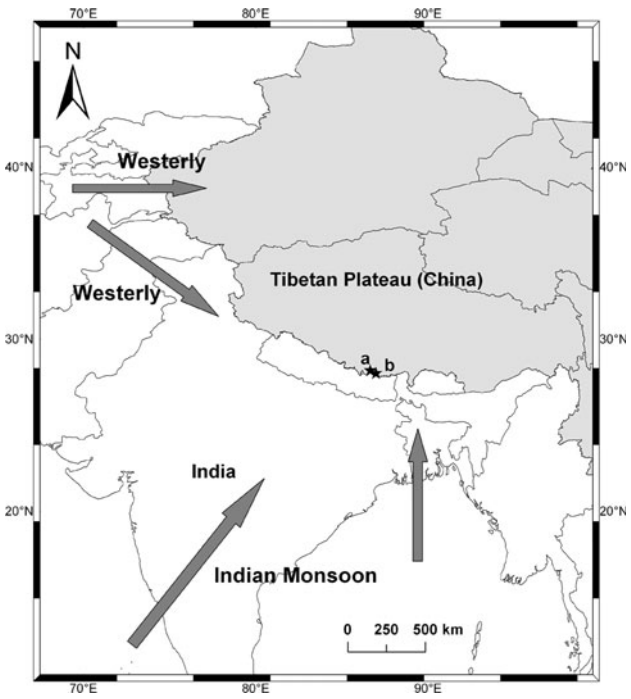

Fig. 1 Sketch map showing snow pits sampling sites at Cho Oyu (*a*) and Mt. Qomolangma (*b*)

0.87 m depth snow pit was hand-dug by operators wearing clean garments and low-density polyethylene (LDPE) gloves. Continuous nine snow pit samples were collected from the snow surface to the bottom at an interval of 10 cm for the upper eight samples and 7 cm for the bottom sample, using ultra-clean cylindrical Teflon containers (diameter 5 cm, length 35 cm), which were hammered horizontally into the wall of the pit. The samples were transferred directly into ultra-clean 500 ml LDPE bottles. The bottles were then packed in double sealed acid-cleaned LDPE bags and kept frozen until analysis. All sampled tools, including scrapers, hammers, cylindrical Teflon containers, and 500 ml LDPE bottles were cleaned at the Korea Polar Research Institute (KOPRI) as described by Hong et al. (2000). In addition, parallel samples for measurements of major ions, oxygen isotopes, and microparticles were also collected at the same interval from the same wall of the snow pit. After sampling, the samples were transported frozen to the State Key Laboratory of Cryospheric Sciences (SKLCS) and the Korea Polar Research Institute.

Chemical measurements

Measurements of trace elements were performed at KOPRI using inductively coupled plasma mass spectrometer (ICP-MS) (Perkin Elmer Sciex, ELAN 6100). The samples were melted at air temperature inside a class 10 clean bench in a class 1,000 clean room. The samples were

Table 1 Detection limit (pg g^{-1}) and analytical results (ng g^{-1}) of certified reference material SLRS-4

Element	Mass no.	Detection limit	Found	Certified
V	51	2.7	0.36 ± 0.004	0.32 ± 0.03
Cr	53	21.4	0.35 ± 0.02	0.33 ± 0.02
Mn	55	1.5	3.39 ± 0.03	3.37 ± 0.18
Co	59	0.5	0.041 ± 0.003	0.033 ± 0.006
Ni	60	2.1	0.78 ± 0.03	0.67 ± 0.08
Cu	63	1.5	1.83 ± 0.08	1.81 ± 0.08
Zn	66	3.3	1.12 ± 0.03	0.93 ± 0.10
As	75	2.6	0.72 ± 0.02	0.68 ± 0.06
Sr	88	0.3	28.3 ± 0.01	26.3 ± 3.2
Cd	114	0.7	0.014 ± 0.001	0.012 ± 0.002
Sn	118	1.2	0.009 ± 0.001	–
Sb	121	0.5	0.24 ± 0.003	0.23 ± 0.04
Ba	138	0.8	12.3 ± 0.1	12.2 ± 0.6
Tl	205	0.1	0.007 ± 0.001	–
Pb	208	0.3	0.083 ± 0.002	0.086 ± 0.007
Bi	209	0.1	0.002 ± 0.001	–
Th	232	0.1	0.02 ± 0.001	–
U	238	0.3	0.050 ± 0.001	0.050 ± 0.003

acidified to 1% with Fisher "Optima" grade ultra-pure HNO_3. The instrument settings, such as quartz cyclonic spray chamber, Pt sampler cone and Pt skimmer cone, were employed to enhance peak sensitivity. The instrument was optimized to obtain the maximum sensitivity and extend stability using a solution of 1 ng g^{-1} Rh and the maximum sensitivity varied between 55,000 and 60,000 counts s^{-1} (cps). External calibration curves were used for quantification.

Detection limits, defined as three times that of the standard deviation of ten measurements of blank solution (1% Fisher "Opitima" grade HNO_3 water solution), are presented in Table 1. The accuracy of the method was verified by analyzing a riverine water reference (SLRS-4, River Water Reference Material for Trace Metals, National Research Council Canada, Ottawa, Canada), and good agreement between the measured and the certified values was observed for most measured elements (Table 1).

Measurements of major ions, oxygen isotopes, and microparticles were performed at SKLCS. Major ions were analyzed by Dionex 300 ion chromatograph (detection limit 1 ng g^{-1}) and oxygen isotopic ratios by Delta-plus mass spectrometer (accuracy 0.05‰). Microparticles were measured by an Accusizer 780 Optical Particle Sizer (Santa Barbara, CA, USA).

Assignment of seasonality to snow deposits

Snow samples are dated by combining the depth profiles of isotope ($\delta^{18}O$), major ion (Ca^{2+}), and microparticles based on the apparent difference between monsoon and non-monsoon seasons.

In the southern Tibetan Plateau and Himalayan region, the mechanism controlling the stable isotopes in precipitation is closely related to the monsoon moisture transport. Strong monsoon activities during summer result in high precipitation rates and more depleted heavy isotope (more negative $\delta^{18}O$) by fractionation, which is commonly referred as the precipitation "amount effect" (Tian et al. 2003). Therefore, the $\delta^{18}O$ depletion occurs during the summer monsoon season, and the $\delta^{18}O$ enrichment is related to westerly air masses during the non-monsoon dry season (fall, winter, and spring) (Thompson et al. 2000; Zhang et al. 2005).

Glaciochemical studies of snow and ice in the central Himalayas have revealed that the concentrations of major ions (e.g., Ca^{2+} and Mg^{2+}) in the monsoon season are generally lower than those in the non-monsoon season, presenting a striking seasonal variation (Shrestha et al. 2000; Kang et al. 2004). Insoluble microparticles in snow and ice are enhanced during the non-monsoon period, especially in spring, due to the strong dust inputs from source regions, while they were low during the monsoon season due to the moisture transport from Indian Ocean (Xu et al. 2007).

The profiles of $\delta^{18}O$, Ca^{2+}, and microparticle concentrations versus depth are presented in Fig. 2. The mean concentration values of $\delta^{18}O$ (−14‰), Ca^{2+} (818 ng g^{-1}), and microparticles (309 10^3/ml) tend to be significantly high in the top 0–30 cm snow layer, representing non-monsoon season deposition. The lower mean values of $\delta^{18}O$ (−21‰), Ca^{2+} (47 ng g^{-1}), and microparticle (37 10^3/ml) concentrations are found between 30 cm and the bottom of snow pit, which can be assigned to the summer monsoon layer in 2005. The snow layers with relatively high values of $\delta^{18}O$, Ca^{2+}, and microparticle concentrations below 70 cm to the bottom of snow pit likely represent the beginning of monsoon season of 2005. By combining well-defined $\delta^{18}O$, Ca^{2+}, and microparticle concentration profiles in these snow samples, the snow pit can be roughly divided into monsoon and non-monsoon seasons marked by the dashed vertical line (Fig. 2), which covers approximately several months from summer to fall of 2005.

Results

The profiles of the trace elements are given in Fig. 3, showing an apparent link between the trace elements and Ca^{2+} and Ba that are derived from mineral dust during the monsoon and non-monsoon seasons.

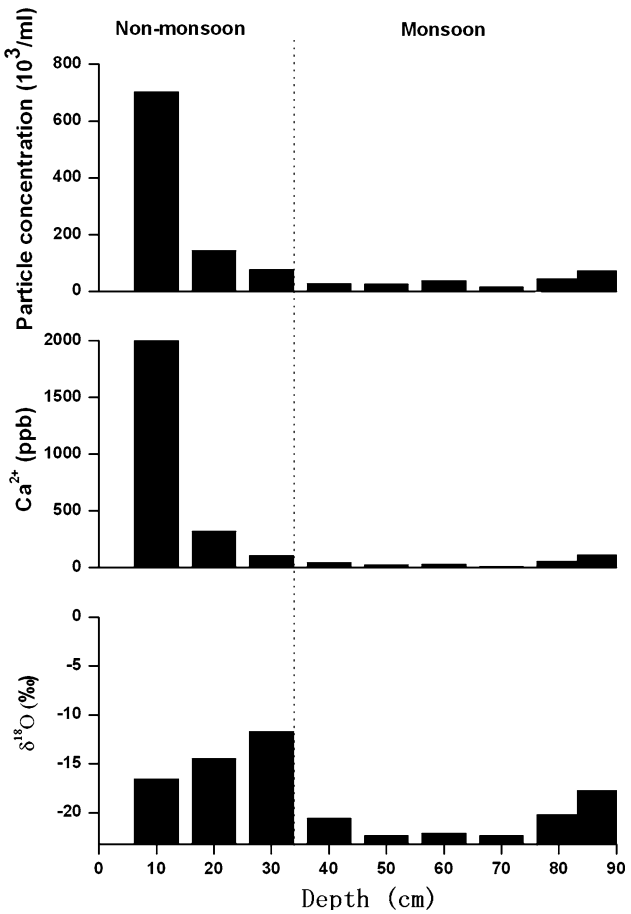

Fig. 2 Depth profiles of $\delta^{18}O$, Ca^{2+} and microparticle concentrations of the Cho Oyu snow pit. *Vertical dashed lines* represent the seasonal boundaries

The statistics of trace elements are summarized in Table 2, indicating that their concentrations differ by orders of magnitude, with the highest values at ng g^{-1} level for Mn, Zn, Rb, Sr, and Ba, and the lowest values at pg g^{-1} for Co, Cd, Sn, Sb, Tl, Th, Bi, and U. The ratios of maximum against minimum concentrations range from 6 for Cr to 48 for Th (Table 2). To distinguish the difference in trace elements between the monsoon and non-monsoon seasons, the mean concentrations of trace elements were calculated during the monsoon season, the non-monsoon season and of all samples, as presented in Table 2. Mean values of all samples varied from 3 pg g^{-1} for Sb to 1.4 ng g^{-1} for Mn.

Discussion

Seasonal variation of trace elements

A distinct difference between the measured trace element concentrations is shown in Table 2 and Fig. 3, with higher concentrations during the non-monsoon season and lower concentrations during the monsoon season. Such a seasonality was also previously observed for major ions, trace elements, and dust in the Himalayan snow and ice (Balerna et al. 2003; Kang et al. 2004; Xu et al. 2007; Lee et al. 2008).

Correlation coefficients of trace elements are presented in Table 3, which can give some insight into the possible sources for the different trace elements (Barbante et al. 2003). Most trace elements have significant correlations

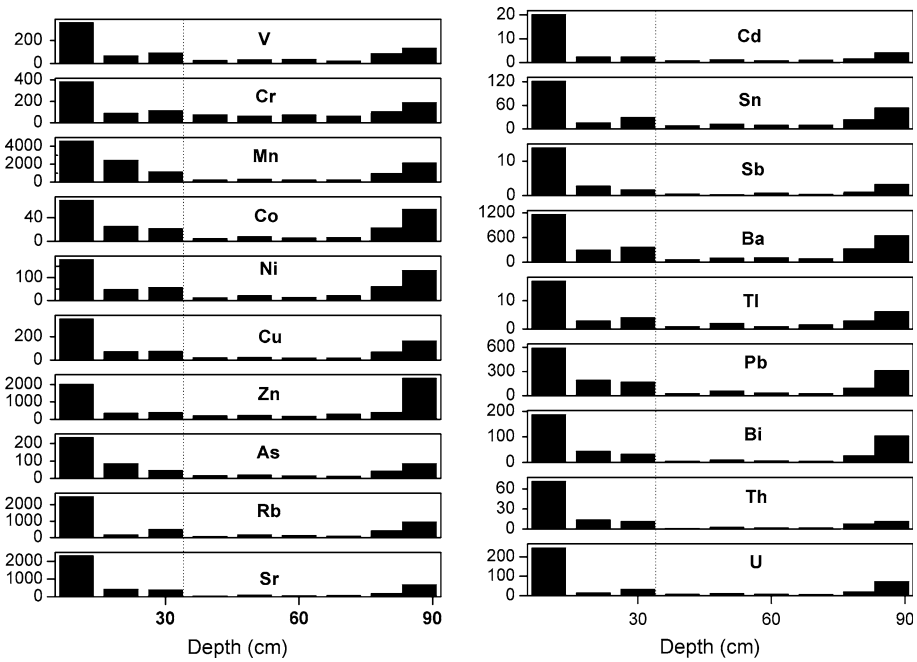

Fig. 3 Profiles of trace elements of the Cho Oyu snow pit. *Vertical dashed lines* represent the seasonal boundaries

Table 2 Statistics of trace elements (pg g^{-1}) of the Cho Oyu snow pit samples

Element	Min.	Max.	Max./min.	Mean value		
				All samples	Monsoon	Non-monsoon
V	26	357	14	97	58	173
Cr	64	382	6	129	96	196
Mn	243	4,598	19	1,383	703	2,742
Co	5	70	14	24	17	39
Ni	13	180	13	61	44	95
Cu	19	353	18	91	53	167
Zn	181	2,375	13	718	616	922
As	14	235	16	62	32	123
Rb	87	2,498	29	572	323	1,068
Sr	68	2,312	34	489	207	1,055
Cd	1	20	26	4	2	8
Sn	9	122	14	32	20	56
Sb	0.5	15	31	3	1	6
Ba	71	1,165	16	356	228	612
Tl	1	17	18	4	2	8
Pb	31	592	19	170	95	319
Bi	6	188	33	47	26	88
Th	1	71	48	14	5	32
U	7	246	33	47	22	98

($P = 0.01$) with Ba (which originates from the rock and soil dust). This suggests that these trace elements originate from a similar mineral dust source and/or similar transport and deposition processes during the non-monsoon and monsoon seasons.

Contribution from natural sources

An assessment of emissions of natural trace elements to the atmosphere for present-day climatic condition indicates that they originate mainly from rock and soil dust, sea salt spray, wild forest fires, volcanoes, and continental and marine biogenic sources (Nriagu 1989). Crustal enrichment factor (EF_c) can be used as an index to evaluate trace elements from soil and rock dust and to assess further the relative contribution from natural versus anthropogenic sources. EF_c is defined as the concentration ratio of a given element to that regarded as a good proxy of rock and soil dust (e.g., Al and Ba), and normalized to the same concentration ratio characteristic of the upper continental crust. For example, the EF_c for Pb is:

$$EF_c = \frac{(Pb/Ba)_{snow}}{(Pb/Ba)_{crust}}$$

The data of upper continental crust given by Wedepohl (1995) were used in this study. EF_c values should be

Table 3 Correlation coefficients of trace elements for the Cho Oyu snow pit samples

	Ba	V	Cr	Mn	Co	M	Cu	Zn	As	Rb	Sr	Cd	Sn	Sb	Tl	Pb	Bi	Tl	U
Ba	1																		
V	0.98	1																	
Cr	0.98	099	1																
Mn	0.94	0.92	0.91	1															
Co	0.97	0.91	0.93	0.93	1														
Ni	0.98	0.94	0.95	0.91	0.99	1													
Cu	0.99	0.99	0.99	0.94	0.95	0.97	1												
Zn	0.86	**0.77**	0.82	**0.75**	0.92	0.92	0.84	1											
As	0.96	0.97	0.96	0.98	0.91	0.91	0.98	**0.74**	1										
Rb	0.97	0.99	1.00	0.89	0.91	0.94	0.99	0.80	0.95	1									
Sr	0.96	0.99	0.98	0.94	0.89	0.91	0.98	**0.75**	0.99	0.98	1								
Cd	0.93	0.98	0.97	0.89	0.84	0.86	0.96	**0.69**	0.97	0.98	0.99	1							
Sn	0.98	0.99	1.00	0.90	0.93	0.95	0.99	0.82	0.96	1.00	0.98	0.97	1						
Sb	0.94	0.98	0.97	0.93	0.86	0.88	0.97	**0.70**	0.98	0.97	1.00	0.99	0.97	1					
Tl	0.97	0.99	0.99	0.92	0.91	0.93	0.99	**0.77**	0.97	0.99	0.99	0.98	0.99	0.98	1				
Pb	0.99	0.97	0.97	0.97	0.96	0.96	0.99	0.84	0.98	0.96	0.97	0.93	0.97	0.95	0.97	1			
Bi	0.99	0.97	0.98	0.95	0.97	0.98	0.99	0.89	0.97	0.97	0.97	0.93	0.98	0.95	0.97	0.99	1		
Th	0.93	0.98	0.96	0.92	0.83	0.85	0.96	**0.65**	0.98	0.96	0.99	0.99	0.96	0.99	0.98	0.94	0.92	1	
U	0.95	0.99	0.99	0.89	0.88	0.91	0.98	**0.77**	0.96	0.99	0.99	0.99	0.99	0.98	0.99	0.95	0.96	0.98	1

The coefficients that are insignificant at 99% confidence level are shown in bold

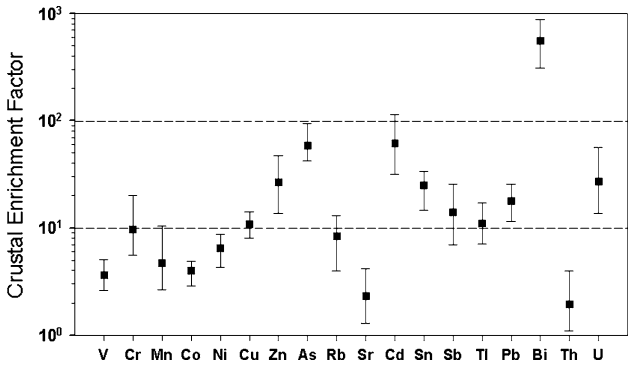

Fig. 4 Mean EF_c for the measured trace elements of the Cho Oyu snow pit samples. The *bars* show the ranges of EF_c values on a logarithmic *y*-scale

qualitatively used in evaluating the relative contribution from rock and soil dust owing to the uncertainty of calculation of EF_c attributed to the differences between chemical composition of local soil and reference crustal composition (Lee et al. 2008). EF_c values less than ~ 10 suggest that the element is derived primarily from rock and soil dust, while EF_c values significantly larger than ~ 10 suggest an important contribution from other natural sources or anthropogenic sources (Barbante et al. 2003).

Figure 4 shows the mean values and ranges of EF_c for all the measured trace elements. The mean EF_c of trace elements are from 2 for Th to 560 for Bi, with a large difference between elements. For V, Cr, Mn, Co, Ni, Rb, Sr, and Th, their mean EF_c values are less than 10, suggesting that these elements originated mainly from rock and soil dust. Among these elements, the highest EF_c values of Cr, Mn, and Rb are more than 10, indicating that contributions from other natural or anthropogenic sources might be important for part of the samples. For Cu, Zn, As, Cd, Sn, Sb, Tl, Pb, Bi, and U, their mean EF_c values are from 11 to 560, suggesting that contributions from other natural or anthropogenic sources might be important for these trace elements. For Cu, Sb, and Tl, their lowest EF_c values are below 10, suggesting that contribution from rock and soil dust is potentially important for part of the samples. Furthermore, the EF_c values for Zn, As, Cd, Sn, Pb, Bi, and U during the monsoon and non-monsoon seasons are all more than 10, suggesting that these trace elements are dominated by other natural or anthropogenic inputs. Trace elements, such as As, Cd, and Bi, show very high EF_c in all samples, suggesting that the crustal dust contribution is always insignificant for these elements.

The contribution from sea-salt spray can be evaluated from Na concentrations measured in the snow and the element to Na ratios in surface ocean water after correction for Na contributed from rock and soil dust (Lee et al. 2008). Na, in these samples, derived mainly from rock and soil dust due to very low Na concentrations (less than detection limit) during monsoon season, was observed. Thus, the sea-salt spray contribution can be negligible.

Volcanoes are significant sources of trace elements to the atmosphere at regional and global scales (Nriagu 1989; Fulignati et al. 2006). Contributions from volcanoes can be estimated from the concentration of non-sea-salt sulphate (nss-SO_4^{2-}) assuming that approximately 10–15% of nss-SO_4^{2-} originated from volcanoes (Boutron and Patterson 1986). However, this approach is not appropriate for these samples due to the nss-SO_4^{2-} at high altitudes of the central Himalayas, which is primarily of crustal origin (Lee et al. 2008 and references therein). Studies suggested that volcanic emissions could be the significant natural source of As, Cd, and Bi (Hong et al. 2005; Gabrielli et al. 2005). As the lowest EF_c values are above 30 for these elements in the samples, it is likely that volcanic contributions for these elements are significant. The volcanic events occurred during 2005 ejected materials into the troposphere that can be transported via atmospheric circulation and deposited on the surface of the snow in the high altitude Himalayan region (Xu et al. 2009a). For example, the eruption of Barren Island volcano (12°16′40″N, 93°51′30″E), India, began on 26 May 2005 and stopped on 23 December 2007 and the eruption column of ash particles attained a height of more than 300 m (Pal et al. 2007).

The contributions from continental and marine biogenic emissions cannot be calculated from these data, because no data on particulate organic carbonate are available for the samples. It is likely that this contribution cannot explain the very large excess above rock and soil dust contribution for most measured trace elements in these samples.

Contribution from anthropogenic sources

The major anthropogenic sources emitting into the atmosphere include fossil fuel combustion, gasoline combustion, non-ferrous metal production, ferrous foundries operations, refuse incineration, and cement production (Pacyna and Pacyna 2001). The large fraction of trace elements such as Cu, Zn, As, Cd, Sn, Sb, Tl, Pb, Bi, and U excess above rock and soil dust contribution in these samples is likely of anthropogenic origin. A comprehensive inventory of anthropogenic emissions of trace elements into the atmosphere has been published (Pacyna and Pacyna 2001). It gives estimates of emissions from different source categories for different continents, for some of the trace elements considered in this work. In Asia, the fossil fuel combustion is the major source of Cr, Sb, Mn, Sn, and Tl, and non-ferrous metal production is the largest source of atmospheric Cd, Cu, As, and Zn. Combustion of leaded, low-leaded and unleaded gasoline is the major source of atmospheric Pb. In addition, Rb and Bi are likely from biomass burning and fossil fuel combustion, respectively (Plessow

et al. 2001; Morawska and Zhang 2002), which were not considered by Pacyna and Pacyna (2001). U is likely from the application of uranium containing phosphate fertilizers (Kratz and Schnug 2006).

Comparison of trace element concentration with other data

To understand the spatial distribution and the current situation of the inputs of trace elements in the Himalayan snow, these results were compared with those of snow samples from Mt. Qomolangma (28°01′08″N, 86°57′48″E, 6,576 m a.s.l.; Fig. 1b) (Lee et al. 2008) and Greenland (72°20′N, 38°45′W, 3,270 m a.s.l.) (Barbante et al. 2003).

As indicated from Table 4, the mean concentrations of crustal elements (V, Cr, Mn, Co, Ni, and Rb) at Cho Oyu are comparable to that at Mt. Qomolangma. The mean concentration of Co at Cho Oyu is four times higher than that at Greenland, possibly due to the proximity of Cho Oyu to source area of dust.

The concentrations of trace elements with an anthropogenic contribution (i.e., Cu, Zn, As, Cd, Sb, Pb, and Bi) are higher at Cho Oyu than those at Mt. Qomolangma; however, their values tend to be similar levels. On the other hand, the concentrations of Cu, Zn, Pb, Bi, and U are about one order of magnitude higher than those at Greenland (as a representative area remote from the anthropogenic pollutant sources), which is expected due to the proximity of Cho Oyu to anthropogenic pollution sources for these elements. Together with high EF_c values observed for these elements in Cho Oyu snow samples, the authors' comparison suggests that high altitude atmosphere in the central Himalayas has been polluted by anthropogenic emissions.

Potential source regions for trace elements at Cho Oyu indicated by air mass trajectories

Because most trace elements are non-volatile and less prone to chemical transformation, they tend to be transported over a long distance and remain in the form they were emitted (Morawska and Zhang 2002). Air backward trajectories are suitable to deduce the potential source regions of trace elements. The hybrid single-particle Lagrangian integrated trajectory (HHSPLIT) model is a tool to simulate air mass trajectories and complex dispersion and deposition (Draxler and Hess 1998). 5-day-back trajectories to simulate the routes of air masses reaching our sampling site at 00:00, 06:00, 12:00, and 18:00 (UTC time) of each day were calculated using HYSPLIT 4.8 model from 1 December 2004 to 30 November 2005. The Climate Diagnostics Center NCEP/NCAR 1 (CDC-1) model data available in NOAA's Air Resource Laboratory (ARL) archives were used. The clustering tool integrated in the model was applied to form clusters of trajectories based on the percentage change in total space variance (TSV) and to calculate the mean backward trajectories of all the trajectories of 2005 (Fig. 5). To investigate seasonal patterns of trajectories, a 1-year dataset was split into four seasons, i.e., the winter (December and January–February), spring (March–May), summer (June–August), and autumn (September–November) (Fig. 5), and the cluster analysis technique was also separately applied to each of the four seasons.

The mean trajectories of winter and spring (Fig. 5) have two main clusters, indicating that the atmosphere over Cho Oyu region is controlled by the westerlies during winter and spring. Cluster 2 represents air masses originating from the Sahara Desert in North African, passing through Iran, Pakistan, and the northwest of India, and arriving finally at our sampling site in about 5 days. When the air masses pass through these regions, dust can be entrained into the atmosphere and stay aloft for a long distance, especially for the fine dust, before being scavenged by precipitation in the Himalayas. This suggests that the trace elements associated with dust loaded on the snow and ice in central Himalayas may not come primarily from the arid and semi-arid regions in central Asia (Mayewski et al. 1986; Wake et al. 1990; Williams et al. 1992), but mainly from the Thar Desert in North India, as well as the regions in West Asia, or even the distant Sahara Desert in North African. This agrees well with other studies which suggested that the long-range transport of desert dust from arid regions ranging from India and the Middle East to perhaps as far as the Sahara was responsible for dust deposition in the central Himalayas (Carrico et al. 2003; Xu et al. 2009b). In summer, the air trajectories originate from several regions

Table 4 Mean concentrations (pg g^{-1}) of the snow samples at Cho Oyu, Qomolangma and Greenland

Location	Time period investigated	Altitude (m)	V	Cr	Mn	Co	Ni	Cu	Zn	As	Rb	Cd	Sb	Pb	Bi	U	References
Cho Oyu	2005	6,303	97	129	1,383	24	61	91	718	62	572	4	3	170	47	47	This study
Qomolangma	2004–2005	6,576	111	104	1,302	36	85	76	475	20	372	2	1	77	5		Lee et al. (2008)
Greenland	1991–1995	3,270				6		5	51			1	1	17	3	2	Barbante et al. (2003)

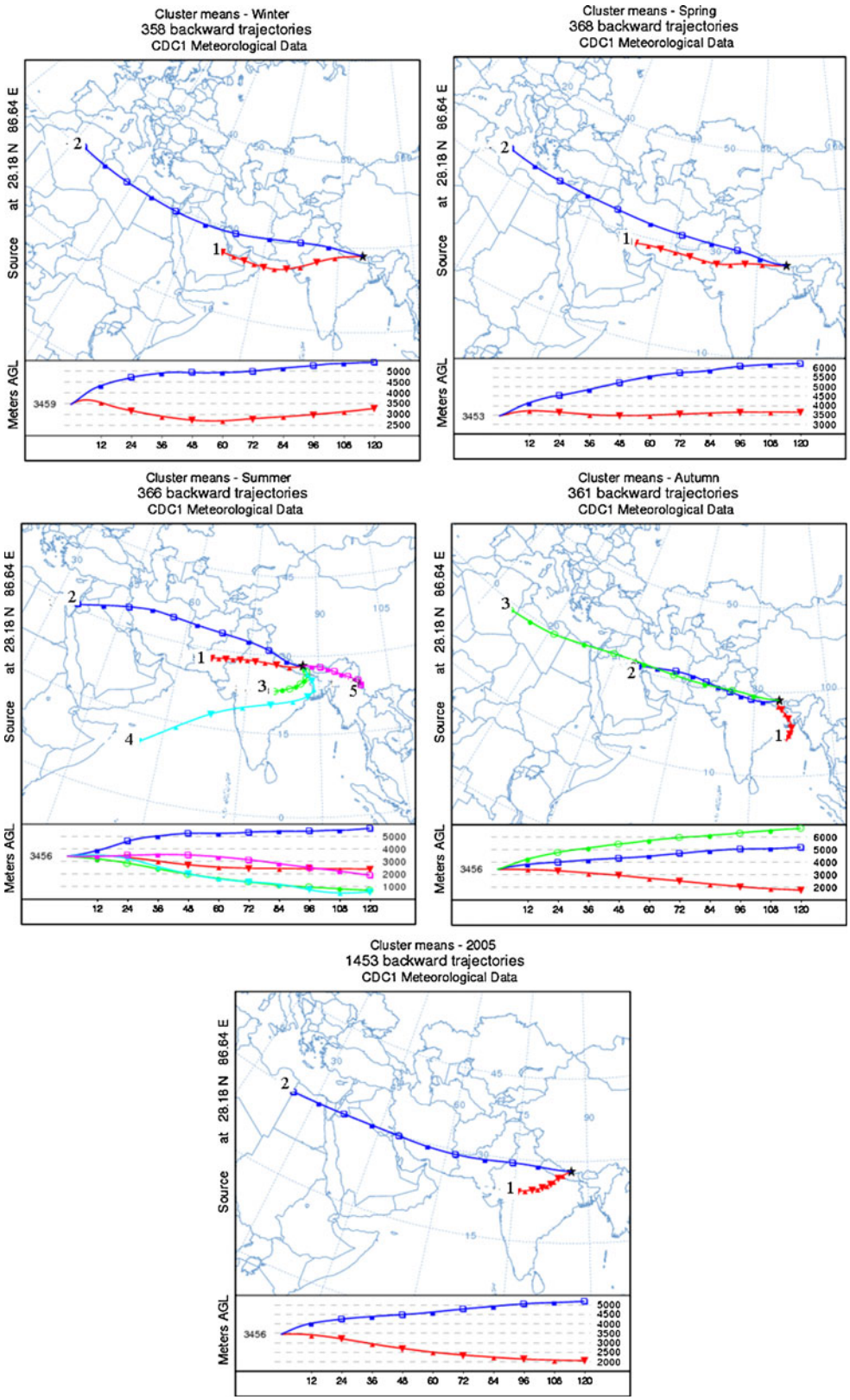

Fig. 5 Mean 5-day-back trajectories with six-hourly resolution reaching the sampling site during each season and the whole year of 2005 simulated by the HYSPLIT 4.8 model. The altitude (3,456 m a.s.l.) represents meter above model ground level and each main cluster is given by a serial number

(Fig. 5). Cluster 2 represents the westerlies over a long distance and clusters 1, 3, 4, and 5 represent trajectories over a local or regional distance. Cluster 1, 3, and 4 represent Indian Monsoon, and cluster 5 represents the Bay of Bengal monsoon. The Indian monsoon water vapor comes from Arabian Sea/India Ocean, and arrives at the

Himalayas a few days later. In autumn, the summer monsoon weakens gradually, and is replaced by the westerlies later. In case of 2005 (Fig. 5), two clusters can be derived directly from the HYSPLIT model. Cluster 1 represents the trajectory of relatively short distance and low elevation by Indian monsoon prevailing during the monsoon season, while cluster 2 represents the trajectory of relatively long distance and high elevation by the westerlies prevailing during the non-monsoon season.

Therefore, the seasonal variation of source regions for atmospheric trace elements in Cho Oyu is pertinent to different atmospheric circulation patterns in central Himalayas. The atmospheric trace elements pollution revealed by these Cho Oyu snow samples results from inputs of anthropogenic trace elements by short or long distance transport from source regions. The rapid economic growth and increasing of agricultural and industrial activities in the source regions (e.g., India) in the recent decades result in serious anthropogenic trace element pollution in the atmosphere (Pacyna and Pacyna 2001; Fang et al. 2005), even in the remote high altitude atmosphere over Cho Oyu region of the central Himalayas.

Conclusions

Trace element concentrations were determined by ICP-MS in snow pit samples from the Gyabrag glacier nearby Cho Oyu. The data show pronounced seasonal variation of concentrations of trace elements accompanying the shift from monsoon and non-monsoon seasons. The concentrations of trace elements present high values during the non-monsoon season and low values during the monsoon season. The analysis of crustal enrichment factors indicates that the contribution from rock and soil dust is probably important for V, Mn, Co, Ni, Rb, Sr, and Th, while anthropogenic inputs may be important sources for trace elements of Cu, Zn, As, Cd, Sn, Sb, Tl, Pb, Bi, and U. The atmospheric transport pathways of trace elements were investigated by the HYSPLIT model, indicating that air masses were transported dominantly by Indian summer monsoon during the monsoon season, while air masses were transported completely by the westerlies during the non-monsoon season.

It will be interesting to expand this study by investigating other trace elements such as Pt, Pd, and Rh, which have been widely dispersed into the atmospheric environment by increasing use of automobile catalytic converters in recent decades. It will be worthwhile to investigate the variation of lead isotopes and organo-lead to identify natural and anthropogenic contributions to the fallout of Pb in this region. Finally, it will be necessary to study long-term records of trace elements in ice cores extracted from Cho Oyu region to assess historical variation of atmospheric pollution of these elements in this region.

Acknowledgments Thanks are due to many scientists, technicians, graduates students, and porters for hard work expertly carried out in the field. The authors greatly appreciate the comments from anonymous reviewers for the improvement of this paper. This work was supported by the Natural Science Foundation of China (40825017), National Basic Research program of China (2007CB411501), the Chinese Academy of Sciences (SKLCS-ZZ-2008-06, 100 Talents Project) and the Nanjing University. In Korea, this work was supported by KOPRI research Grant (PP09010) and INHA University Research Grant (INHA-40890-01).

References

Balerna A, Bernieri E, Pecci M, Polesello S, Smiraglia C, Valsecchi S (2003) Chemical and radio-chemical composition of freshsnow samples from northern slope of Himlayas. Atmos Environ 37:1573–1581

Barbante C, Boutron C, Morel C, Ferrari C, Jaffrezo J, Cozzi G, Gaspari V, Cescon P (2003) Seasonal variations of trace elements in central Greenland snow deposited from 1991 to 1995. J Environ Monit 5:328–335

Barbante C, Schwikowski M, Doring T, Gaggeler HW, Schotterer U, Tobler L, Vande Valde K, Ferrari C, Cozzi G, Turetta A, Rosman K, Bolshov M, Capodaglio G, Cescon P, Boutron C (2004) Historical record of European emissions of trace elements to the atmosphere since the 1650s from alpine snow/ice cores drilled near Monte Rosa. Environ Sci Technol 38:4085–4090

Boutron CF, Patterson CC (1986) Lead concentration changes in Antarctic ice during the Wisconsin/Holocene transition. Nature 323:222–225

Boutron CF, Görlach U, Candelone JP, Bolshov MA, Delmas RJ (1991) Decrease in anthropogenic lead, cadmium and zinc in Greenland snows since the late 1960s. Nature 353:153–156

Candelone JP, Hong S, Pellone C, Boutron CF (1995) Industrial revolution changes in large-scale atmospheric pollution of the Northern Hemisphere for trace elements as documented in central Greenland snow and ice. J Geophys Res 100:16605–16616

Carrico CM, Bergin MH, Shrestha AB, Dibb Jack E, Gomes L, Harris JM (2003) The importance of carbon and mineral dust to seasonal aerosol properties in the Nepal Himalaya. Atmos Environ 37:2811–2824

Draxler RR, Hess GD (1998) An overview of the HYSPLIT-4 modelling system for trajectories, dispersion, and deposition. Aust Meteorol Mag 47:295–308

Duan J, Ren J, Qin X, Li Y (2007) Trace element concentrations and seasonal variations in snow of Mount Everest Region. Acta Geogr Sin 62(1):22–29 (In Chinese)

Fang G, Wu Y, Huang S, Rau J (2005) Review of atmospheric metallic elements in Asia during 2000–2004. Atmos Environ 39:6420–6429

Foell W, Green C, Amann M, Bhattacharya S, Carmichael G, Chadwick M, Cinderby S, Haugland T, Hettelingh J-P, Hordijk L, Kuylenstierna J, Shah J, Shrestha R, Streets D, Zhao D (1995) Energy use, emissions, and air pollution reduction strategies in Asia. Water Air Soil Pollut 85:2277–2282

Fulignati P, Sbrana A, Clocchiatti R, Luperini W (2006) Environmental impact of the acid fumarolic plume of passively degassing volcano (Vulcano Island, Italy). Environ Geol 49:1139–1155

Gabrielli P, Barbante C, Boutron CF, Cozzi G, Gaspari V, Planchon F, Ferrari C, Turetta C, Hong S, Cescon P (2005) Variations in atmospheric trace elements in Dome C (East Antarctica) ice over the last two climatic cycles. Atmos Environ 39:6420–6429

Hong S, Candelone JP, Patterson CC, Boutron CF (1994) Greenland ice evidence of hemispheric scale pollution for lead two millennia ago by Greek and Roman civilizations. Science 265:1841–1843

Hong S, Candelone JP, Patterson CC, Boutron CF (1996) History of ancient copper smelting pollution during Roman and Medieval times recorded in Greenland ice. Science 272:246–249

Hong S, Lluberas A, Rodriguez F (2000) A clean protocol for determining ultralow trace element concentrations: its application to the analysis of Pb, Cd, Cu, Zn and Mn in Antarctic snow. Kor J Polar Res 11:35–47

Hong S, Barbante C, Boutron CF, Gabrielli P, Gaspari V, Cescon P, Thompson L, Ferrari C, Francou B, Maurice-Bourgoin L (2004) Atmospheric trace elements in tropical South America during the past 22,000 years recorded in a high altitude ice core from Sajama, Bolivia. J Environ Monit 6:322–326

Hong S, Boutron C, Barbante C, Hur SD, Lee K, Gabrielli P, Capodaglio C, Ferrari CP, Turetta C, Petit JR, Lipenkov V (2005) Glacial-interglacial changes in the occurrence of Pb, Cd, Cu and Zn in Vostok Antarctic ice from 240,000 to 410,000 years BP. J Environ Monit 7:1326–1331

Kang S, Mayewski P, Qin D, Sneed SA, Ren J, Zhang D (2004) Seasonal differences in snow chemistry from the vicinity of Mt. Everest, central Himalayas. Atmos Environ 38:2819–2829

Kang S, Zhang Q, Kaspari S, Qin D, Cong Z, Ren J, Mayewski P (2007) Spatial and seasonal variations of elemental composition in Mt. Everest (Qomolangma) snow/firn. Atmos Environ 41:7208–7218

Kratz S, Schnug E (2006) Rock phosphates and P fertilizers as sources of U contamination in agricultural soils. In: Merkel B (ed) Uranium in the environment: mining impact and consequences. Springer, Heidelberg, pp 57–67

Lee K, Hur SD, Hou S, Hong S, Qin X, Ren J, Liu Y, Rosman KJR, Barbante C, Boutron C (2008) Atmospheric pollution for trace elements in the remote high-altitude atmospher in central Asia as recoreded in snow from Mt. Qomolangma (Everest) of the Himalayas. Sci Total Environ 404:171–181

Li Y, Yao T, Wang L, Li Z, Tian L, Xu B, Wu G (2006a) Recent changes of atmospheric trace elements in a high-elevation ice core from Muztagh Ata, east Pamirs: initial results. Ann Glaciol 43:154–159

Li Z, Yao T, Tian L, Xu B, Li Y (2006b) Atmospheric Pb variations in central Asia since 1955 from Muztagata ice core record, eastern Pamirs. Chin Sci Bull 51:1996–2000

Li ZQ, Li C, Li Y, Wang F, Li H (2007) Preliminary results from measurements of selected trace metals in the snow-firn pack on Ürümqi glacial No. 1, eastern Tien Shan, China. J Glaciol 53:368–373

Mayewski PA, Lyons WB, Spencer MJ, Clayton JL (1986) Snow chemistry from Xixabanma Peak, Tibet. J Glaciol 32:542–543

Morawska L, Zhang J (2002) Combustion sources of particles.1. Health relevance and source signatures. Chemosphere 49(9): 1045–1058

Murozumi M, Chow TJ, Patterson CC (1969) Chemical concentrations of pollutant aerosols, terrestrial dusts and sea salts in Greenland and Antarctic snow strata. Geochim Cosmochim Acta 33:1247–1294

Nriagu JO (1989) A global assessment of natural sources of atmospheric trace metals. Nature 338:47–49

Pacyna JM, Pacyna EG (2001) An assessment of global and regional emissions of trace metals to the atmosphere from anthropogenic sources worldwide. Environ Rev 9:269–298

Pal T, Bandopadhyay P, Mitra S, Raghav S (2007) The 2005 eruption of Barren Volcano: an explosive inner arc volcanism in Andaman Sea. J Geol Soc Ind 69:1195–1202

Planchon FAM, Boutron CF, Barbante C, Cozzi G, Gaspari V, Wolff EW, Ferrari CP, Cescon P (2002) Changes in trace elements in Antarctic snow from Coats Land since the mid-19th to the late-20th century. Earth Planet Sci Lett 200:207–222

Plessow K, Acker K, Heinrichs H, Moller D (2001) Time study of trace elements and major ions during two cloud events at the Mt. Brocken. Atmos Environ 35:367–378

Rosman KJR, Ly C, Van de Velde K, Boutron CF (2000) A two century record of lead isotopes in high altitude alpine snow and ice. Earth Planet Sci Lett 176:413–424

Shrestha AB, Wake CP, Dibb JE, Mayewski P, Whitlow S (2000) Seasonal variations in aerosol concentrations and compositions in the Nepal Himalaya. Atmos Environ 34:3349–3363

Stravisi F, Verza GP, Tartari G (1998) Meteorology and Climatology at high altitude in Himalaya. In: Baudo R (ed) Top of the world environmental research: Mount Everest–Himalayan ecosystem. Ecovision world monograph series. Backhuys Publishers, Leiden, pp 101–122

Tian L, Yao T, Schuster PF, White JWC, Ichiyanagi K, Pendall E, Pu J, Yu W (2003) Oxygen-18 concentrations in recent precipitation and ice cores on the Tibetan Plateau. J Geophys Res 108(D9):4293–4302

Thompson LG, Yao T, Mosley-Thompson E, Davis ME, Henderson KA, Lin PN (2000) A high-resolution millennial record of the South Asian Monsoon from Himalayan ice core. Science 289:1916–1919

Vallelonga P, Van de Velde K, Candelone JP, Morgan VI, Boutron CF, Rosman KJR (2002) The lead pollution history of Law Dome, Antarctica, from isotopic measurements on ice cores: 1500 AD to 1989 AD. Earth Planet Sci Lett 204:291–306

Van de Velde K, Boutron C, Ferrari C, Bellomi T, Barbante C, Rudnev S, Bolshov M (1998) Seasonal variations of trace elements in the 1960s Alpine ice: sources versus meteorological factors. Earth Planet Sci Lett 164:521–533

Wake CP, Mayewski PA, Spencer MJ (1990) A review of central Asian Glaciochemical data. Ann Glaciol 14:301–306

Wedepohl KH (1995) The composition of the continental crust. Geochim Cosmochim Acta 59:1217–1232

Williams MW, Tonnesen KA, Melack JM, Yang D (1992) Sources and spatial variation of the chemical composition of snow in the Tien Shan, China. Ann Glaciol 16:25–32

Wolff EW, Suttie ED, Peel DA (1999) Antarctic snow record of cadmium, copper, and zinc content during the twentieth century. Atmos Environ 33:1535–1541

Xu J, Hou S, Qin D, Kang S, Ren J, Ming J (2007) Dust storm activity over the Tibetan Plateau recorded by a shallow ice core from the north slope of Mt. Qomolangma (Everest), Tibet-Himal region. Geophys Res Lett 34:L17054

Xu J, Kaspari S, Hou S, Kang S, Qin D, Ren J, Mayewski P (2009a) Records of volcanic events since AD 1800 in the East Rongbuk ice core from Mt. Qomolangma. Chin Sci Bull 54(8):1411–1416

Xu J, Hou S, Chen F, Ren J, Qin D (2009b) Trace the sources of particles in the East Rongbuk ice core from Mt. Qomolangma. Chin Sci Bull 54(10):1781–1785

Zhang D, Qin D, Hou S, Kang S, Ren J, Mayewski PA (2005) Climatic significance of record from an 80.36 m ice core in the East Rongbuk Glacier, Mount Qomolangma (Everest). Sci China D 48(2):266–272